Effect of Network Structure on the Stability Margin of Large Vehicle Formation with Distributed Control

He Hao, Prabir Barooah and J.J.P. Veerman

***Abstract*— We study the problem of distributed control of a large network of double-integrator agents to maintain a rigid formation. A few lead vehicles are given information on the desired trajectory of the formation; while every other vehicle only uses information on relative position and velocity from a few other vehicles to compute its control, which are called its neighbors. A predetermined information graph defines the neighbor relationships. We limit our attention to information graphs that are D-dimensional lattices, and examine the stability margin of the closed loop, which is measured by the real part of the least stable eigenvalue of the state matrix. The stability margin is shown to decay to 0 as $O(1/N^{2/D})$ when the graph is "square", where N is the number of agents. Therefore, increasing the dimension of the information graph can improve the stability margin by a significant amount. For a non-square information graph, the stability margin can be made independent of N by choosing the "aspect ratio" appropriately. An information graph with large D may require nodes that are physically apart to exchange information. Similarly, choosing an aspect ratio to improve stability margin may entail an increase in the number of lead vehicles. These results are useful to the designer in making trade-offs between performance and cost in designing information exchange architectures for decentralized control.**

I. Introduction

We consider the problem of formation control of vehicles so that neighboring vehicles maintain a constant prespecified spacing while in motion. This problem is relevant to a number of applications such as formation flying of aerial, ground, and autonomous vehicles for surveillance, reconnaissance, mine-sweeping, etc. [1], [2], [3]. A few lead vehicles are provided information on their desired trajectories that they use in computing their control actions; while the rest of the vehicles are allowed to use only locally available information. In a distributed control architecture, each vehicle can measure only the relative position and velocity with respect to a number of *neighbors*. The neighbor relationship is predefined in terms of a graph, which we call the *information graph*.

The one-dimensional version of this problem, in which a string of vehicles moving in a straight line have to be controlled to maintain a constant inter-vehicle separation, has been extensively studied [4], [5], [6]. The general trend of the results is that the problem scales poorly with the number of vehicles: as the number of vehicles increase the sensitivity to disturbances increases [7], [8], [9] and the stability margin decays [10], [6]. The information graphs considered in the literature are usually limited to at most two neighbors, with notable exceptions such as [11], [14] that consider more general information exchange architectures.

Our goal is to examine how the stability margin scales with the size of the formation and the structure of the information graph that specifies allowable information exchange between pairs of vehicles. The real part of the least stable eigenvalue is used as a measure of the stability margin. The stability margin determines the decay rate of initial formation keeping errors. Such errors arise from poor initial arrangement of the vehicles. In this paper we limit our attention to a specific class of information graphs, namely, D-dimensional (finite) lattices. These are natural choices for information graphs in 2D or 3D formation problems in which vehicles are arranged in regular pattern and relative measurements are possible among physically closest vehicles.

Each vehicle is modeled as a double integrator, and a distributed control algorithm is studied in which every vehicle (except for a few lead vehicles) use only relative position and relative velocity with respect to its neighbors in the information graph. We show that when the network is homogeneous and symmetric (all vehicles use the same control gains and information from each neighbor is given equal weight), the stability margin decays to 0 as $O(1/N^{2/D})$ when the graph is "square". Therefore, increasing the dimension (which may need nodes physically apart to exchange information) of the information graph can improve the stability margin by a considerable amount. For non-square information graph, the stability margin can be made independent of the number of agents by choosing the "aspect ratio" appropriately. That may entail an increase in the number of lead vehicles that have access to the formation's desired trajectory.

The results in this paper are a generalization of the results in [13], which showed that the stability margin when the information graph is a 2-D lattice decays to 0 as $O(1/N)$. The results in [13] were obtained by using the PDE approximation by taking the continuum limit when the number of vehicles is large. In this paper we avoid such approximation, and establish the scaling laws of the stability margin for general D-dimensional lattices. In addition, [13] considered the scenario in which the desired trajectory of the formation was one with a constant velocity, and

H. Hao and P. Barooah are with Department of Mechanical and Aerospace Engineering, University of Florida, Gainesville, FL 32611, USA. email: hehao,pbarooah@ufl.edu. Their work is supported by the National Science Foundation under Grant CNS-0931885 and by the Institute for Collaborative Biotechnologies through grant DAAD19-03-D-0004.

J.J.P. Veerman is with Fariborz Maseeh Department of Mathematics and Statistics, Portland State University, Portland, OR 97201, USA. email: veerman@pdx.edu

moreover, every vehicle knew this velocity. In contrast, the control law we consider requires agents to know only the desired inter-agent separation; the overall trajectory information is made available only to the lead vehicles. This makes the model more applicable to practical formation control applications in which the formation may be required to accelerate or decelerate occasionally, and the decision to do so is made available only to the lead vehicles. Our results have some interesting connections with those in [14], which are discussed at the end.

The rest of this paper is organized as follows. Section II presents the distributed formation control problem. Section III describes the technical results, including one on eigenvalues of a grounded Laplacian matrix that plays a pivotal role on establishing the main result. The main result and its implications are presented in Section IV.

II. Problem statement

We consider the formation control of N identical vehicles, where the position of each vehicle is a D_s-dimensional vector (with $D_s = 1, 2$ or 3); D_s is referred to as the *spatial dimension* of the formation. Let $p_i^{(\mathrm{d})} \in \mathbb{R}$ be the d-th coordinate of the i-th vehicle's position, whose dynamics are modeled by a double integrator:

$$\ddot{p}_i^{(\mathrm{d})} = u_i^{(\mathrm{d})}, \quad \mathrm{d} = 1, \ldots, D_s, \tag{1}$$

where $u_i^{(\mathrm{d})} \in \mathbb{R}$ is the control input (acceleration or deceleration command). The underlying assumption is that each of the D_s coordinates of a vehicle's position can be independently actuated. We say that the vehicles are *fully actuated*. The spatial dimension D_s is 1 for a platoon of vehicles moving in a straight line, and $D_s = 2$ for a formation of ground vehicles.

The control objective is to make the group of vehicles track a pre-specified reference trajectory while maintaining a desired formation geometry. Reference trajectory information is available only to a set of *lead vehicles*. This information is represented by introducing *fictitious reference* vehicles, one for each lead vehicle. Each reference vehicle perfectly tracks its own desired trajectory. Each lead vehicle can measure its relative position and velocity with respect to its corresponding reference vehicle, which is equivalent to lead vehicles having knowledge of the desired trajectory of the formation. Denoting the number of reference vehicles by N_r, the set $\mathbf{V} := \{1, \ldots, N, N+1, \ldots, N+N_r\}$ is the set of all *nodes* in the formation, including N real vehicles and N_r fictitious reference vehicles. The desired formation geometry is specified by a desired relative position vector $\Delta_{i,j}$ for *every* pair of vehicles $(i, j) \in \mathbf{V} \times \mathbf{V}$, where $\Delta_{i,j}$ is the desired value of $p_i(t) - p_j(t)$. The desired inter-vehicular spacings have to be specified in a mutually consistent fashion, i.e., we must have $\Delta_{i,j} = \Delta_{i,k} + \Delta_{k,j}$ for every triple $i, j, k \in \mathbf{V}$. Since we are interested in rigid formations that do not change shape over time, $\Delta_{i,j}$'s are constants. To maintain a rigid formation, the control must make every vehicle track its desired trajectory. The desired trajectory of a real vehicle i, denoted by $p_i^*(t)$ can be uniquely determined from the trajectories of the reference vehicles and the desired formation geometry. In particular, $p_i^*(t) = p_j^*(t) + \Delta_{i,j}$ where j is any reference vehicle, and $p_j^*(t)$ is its trajectory.

Next we define an *information graph* that makes it convenient to describe distributed control architectures.

Definition 1: An *information graph* is an undirected graph $\mathbf{G} = (\mathbf{V}, \mathbf{E})$. The set of edges $\mathbf{E} \subset \mathbf{V} \times \mathbf{V}$ specify which pairs of nodes (vehicles) are allowed to exchange information to compute their local control actions. Two nodes i and j are called *neighbors* if $(i, j) \in \mathbf{E}$, and the set of neighbors of i are denoted by $\mathcal{N}_i$. □

In this paper we consider the following *distributed* control law, whereby the control action at a vehicle depends on the relative position and velocity measurements with its neighbors in the information graph:

$$u_i^{(\mathrm{d})} = \sum_{j \in \mathcal{N}_i} -k(p_i^{(\mathrm{d})} - p_j^{(\mathrm{d})} - \Delta_{i,j}^{(\mathrm{d})}) - b(\dot{p}_i^{(\mathrm{d})} - \dot{p}_j^{(\mathrm{d})}) \tag{2}$$

where $i \in \{1, \ldots, N\}$ on the left hand side and $j \in \mathbf{V}$ on the right hand side. The positive constants k, b are the position and velocity feedback gains, respectively. It is assumed that vehicle i knows its own neighbors (the set $\mathcal{N}_i$), and the desired spacing $\Delta_{i,j}^{(\mathrm{d})}$. If j is a reference vehicle, $p_j^{(d)}(t) = p_j^{(d)*}(t)$, where $p_j^{(d)*}(t)$ is the d-th coordinate of its reference trajectory.

Example 1: Consider the two formations shown in Figure 1 (a) and (b). Their spatial dimensions are $D_s = 1$ and $D_s = 2$, respectively. The information graph, however, is the same in both cases: $\mathbf{V} = \{1, 2, \ldots, 9\}$, $\mathbf{E} = \{(1,2), (1,3), \cdots, (5,6), (6,9)\}$. A drawing of the information graph appears in Figure 1 (c).

In this paper we restrict ourselves to a specific class of information graphs, namely a finite rectangular lattice:

Definition 2 (D-dimensional lattice): A D-dimensional lattice, specifically a $n_1 \times n_2 \times \cdots \times n_D$ lattice, is a graph with $n_1 n_2 \ldots n_D$ nodes, denoted by $\mathbf{Z}_{n_1 \times n_2 \cdots \times n_D}$. □

Figure 2 depicts two examples of lattices. A D-dimensional lattice is drawn in $\mathbb{R}^D$ with a Cartesian reference frame whose axes are denoted by $x_1, x_2, \ldots, x_D$. Note that these coordinate axes may not be related to the coordinate axes in the physical space $\mathbb{R}^{D_s}$. We also define N_d $(d = 1, \ldots, D)$ as the number of real vehicles in the x_d direction. Then we have the relation $N_1 N_2 \ldots N_D = N$ and $n_1 n_2 \ldots n_D = N + N_r$.

We assume that there is at least one boundary every node of which is a reference vehicle. Reference vehicles are only placed on the boundaries; this typically corresponds to lead vehicles being the outermost vehicles in a formation. We call such a boundary a *Dirichlet boundary*. A boundary of the information graph is either a Dirichlet boundary, in which case all nodes on it are reference vehicles, or none of the nodes on it are reference vehicles.

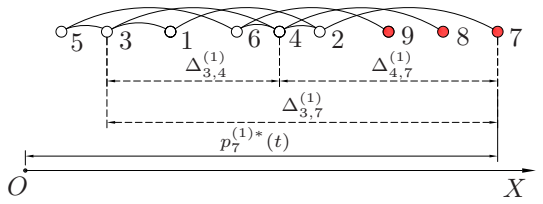

(a) The desired formation geometry of a 1D spatial platoon with 6 vehicles and 3 reference vehicles.

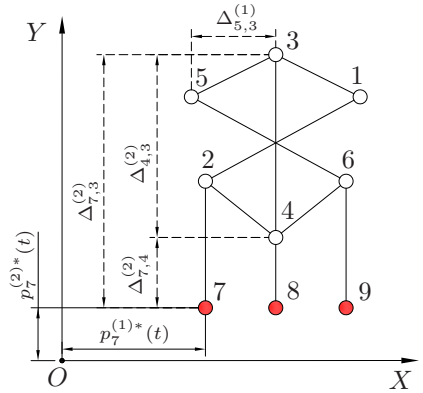

(b) The desired formation geometry of a 2D spatial vehicle formation with 6 vehicles and 3 reference vehicles.

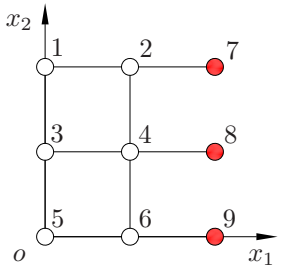

(c) The information graph for both the 1D platoon and the 2D formation shown in (a) and (b).

Fig. 1. (a, b): Two distinct spatial formations that have the same associated information graph (c). Red (filled) circles represent reference vehicles and black (unfilled) circles represent "real" vehicles. Dashed lines (in (a), (b)) represent desired relative positions, while solid lines represent edges in the information graph.

For different configuration of Dirichlet boundaries, N_d and n_d has a slightly different but straightforward relation. For example, in Figure 1 (c), $N_1 + 1 = n_1$ since the boundary perpendicular to the positive x_1 axis is a Dirichlet boundary, while $N_2 = n_2$ since both boundaries perpendicular to the x_2 axis are not Dirichlet boundaries. For a given N, the choice of D and $N_d, n_d, d = 1, \dots D$ specifies the choice of the information graph and its boundary condition.

Remark 1: The dimension D of the information graph is distinct from the spatial dimension D_s. Figure 1 shows an example of two formations in space, one with $D_s = 1$ and the other with $D_s = 2$. The information graph for both the formations is the same 3×3 two-dimensional lattice, i.e., $D = 2$. On account of the fully actuated dynamics and independence of control gains on d, the spatial dimension D_s plays no role in the results of this paper. The dimension of the information graph D, on the other hand, will be shown to play a crucial role.

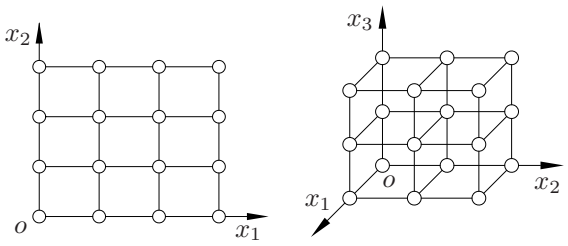

(a) A 2D 4×4 lattice. (b) A 3D $2 \times 3 \times 3$ lattice.

Fig. 2. Examples of 2D and 3D lattices.

III. Stability Margin and Grounded Laplacian

The dynamics of the i-th vehicle are obtained by combining the open loop dynamics (1) with the control law (2), which yields (suppressing the superscript d)

$$\ddot{p}_i = \sum_{j \in \mathcal{N}_i} -k(p_i - p_j - \Delta_{i,j}) - b(\dot{p}_i - \dot{p}_j). \tag{3}$$

To facilitate analysis, we define the following tracking error:

$$\tilde{p}_i(t) := p_i(t) - p^*_i(t), \tag{4}$$

where $p^*_i(t)$ is the i-th agent's desired trajectory. Note that for a rigid formation to be possible, the desired trajectories must satisfy $\dot{p}^*_i - \dot{p}^*_j = 0$ for every i, j, which means $\dot{p}_i - \dot{p}_j = \dot{\tilde{p}}_i - \dot{\tilde{p}}_j$. Therefore, substituting (4) into (3), we have

$$\ddot{\tilde{p}}_i = \sum_{j \in \mathcal{N}_i} -k(\tilde{p}_i - \tilde{p}_j) - b(\dot{\tilde{p}}_i - \dot{\tilde{p}}_j). \tag{5}$$

Since the trajectory of a reference vehicle is assumed to be equal to its desired trajectory, $\tilde{p}_i = 0$ if i is a reference vehicle. To express the closed-loop dynamics of the formation compactly, we define the following state:

$$x := [\tilde{p}_1, \dot{\tilde{p}}_1, \tilde{p}_2, \dot{\tilde{p}}_2, \cdots, \tilde{p}_N, \dot{\tilde{p}}_N]^T$$

Using (5), the state-space model of the vehicle formation can now be written compactly as:

$$\dot{x} = \mathbf{A}x \tag{6}$$

where $\mathbf{A}$ is the closed-loop state matrix.

Definition 3: The *stability margin* is the absolute value of the real part of the least stable eigenvalue of the state matrix $\mathbf{A}$ in (6). □

To facilitate analysis, we define the matrices A_1, A_2 and L_g, where

$$A_1 = \begin{bmatrix} 0 & 1 \\ 0 & 0 \end{bmatrix}, \quad A_2 = \begin{bmatrix} 0 & 0 \\ -k & -b \end{bmatrix}, \tag{7}$$

and L_g is the *grounded (or Dirichlet) Laplacian* matrix of the information graph with reference nodes defining the grounded nodes. To precisely define this matrix recall that

the Laplacian matrix of a graph $\mathbf{G} = (\mathbf{V}, \mathbf{E})$ with n nodes is defined as

$$[L_{n\times n}]_{ij} = \begin{cases} deg(i) & i = j \\ -1 & (i,j) \in \mathbf{E} \\ 0 & \text{otherwise.} \end{cases} \tag{8}$$

where $deg(i)$ is the number of neighbors of node i in the graph. The *grounded* Laplacian L_g matrix of $\mathbf{G}$ with respect to a set of grounded nodes $\mathbf{V}_g \subset \mathbf{V}$ is the submatrix of L obtained by removing from L those rows and columns corresponding to the grounded nodes in $\mathbf{V}_g$. This matrix occurs in the numerical solution of PDEs with Dirichlet boundary conditions and analysis of electrical networks [15]. For example, the grounded graph Laplacian of the information graph shown in Figure 1 (c), with nodes $7, 8, 9$ as the grounded nodes, is:

$$L_g = \begin{array}{c} \\ 1 \\ 2 \\ 3 \\ 4 \\ 5 \\ 6 \end{array} \begin{array}{c} \begin{array}{cccccc} 1 & 2 & 3 & 4 & 5 & 6 \end{array} \\ \begin{bmatrix} 2 & -1 & -1 & 0 & 0 & 0 \\ -1 & 3 & 0 & -1 & 0 & 0 \\ -1 & 0 & 3 & -1 & -1 & 0 \\ 0 & -1 & -1 & 4 & 0 & -1 \\ 0 & 0 & -1 & 0 & 2 & -1 \\ 0 & 0 & 0 & -1 & -1 & 3 \end{bmatrix} \end{array}. \tag{9}$$

It is straightforward to show that

$$\mathbf{A} = I_N \otimes A_1 + L_g \otimes A_2, \tag{10}$$

where I_N is the $N \times N$ identity matrix and $\otimes$ is the Kronecker product.

Theorem 1: The spectrum of $\mathbf{A}$ is

$$\sigma(\mathbf{A}) = \bigcup_{\lambda_\ell \in \sigma(L_g)} \{\sigma(A_1 + \lambda_\ell A_2)\}, \tag{11}$$

$$= \bigcup_{\lambda_\ell \in \sigma(L_g)} \{\sigma \begin{bmatrix} 0 & 1 \\ -k_0\lambda_\ell & -b_0\lambda_\ell \end{bmatrix}\}, \tag{12}$$

where $\sigma(\cdot)$ is the set of distinct eigenvalues. □

Proof of Theorem 1. The proof follows the analysis in [16]. From Schur's triangularization theorem, every square matrix is unitarily similar to an upper-triangular matrix, therefore, there exists an unitary matrix U such that $U^{-1}L_gU = L_u$, where L_u is an upper-triangular matrix, whose diagonal entries are the eigenvalues of L_g. We now do a similarity transformation on matrix $\mathbf{A}$,

$$\begin{aligned} \tilde{\mathbf{A}} =& (U^{-1} \otimes I_2)\mathbf{A}(U \otimes I_2) \\ =& (U^{-1} \otimes I_2)(I_N \otimes A_1 + L_g \otimes A_2)(U \otimes I_2) \\ =& I_N \otimes A_1 + L_u \otimes A_2, \end{aligned}$$

which is a block upper-triangular matrix, and the block on each diagonal is $A_1 + \lambda_\ell A_2$, where $\lambda_\ell \in \sigma(L_g)$. Since similarity transformation preserves eigenvalues, and the eigenvalues of a block upper-triangular matrix are the union of eigenvalues of each block on the diagonal, we complete the proof. ■

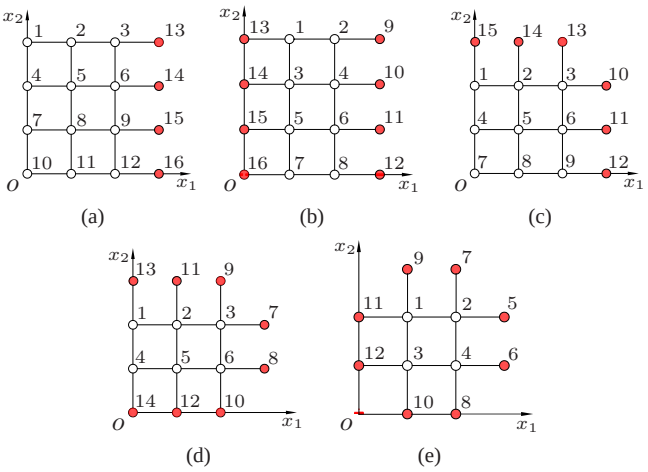

Fig. 3. A pictorial representation of the possible Dirichlet boundary configurations for a 2D information graph.

The next theorem, whose proof is provided in the Appendix, gives an explicit formula for the eigenvalues of the grounded Laplacian for the graphs considered in this paper.

Theorem 2: The eigenvalues of the grounded graph Laplacian L_g of a D-dimensional information graph $\mathbf{Z}_{n_1\times\ldots n_D}$ are positive and are given by the following formula

$$\lambda_\ell := \lambda_{\ell_1,\ldots,\ell_D} = 2D - 2\sum_{d=1}^{D}\Big[I_0(x_d)\cos\frac{(\ell_d-1)\pi}{N_d} + I_1(x_d)\cos\frac{(2\ell_d-1)\pi}{2N_d+1} + I_2(x_d)\cos\frac{\ell_d\pi}{N_d+1}\Big] > 0, \tag{13}$$

where $\ell_d = 1, \ldots, N_d$ $(d = 1, \ldots, D)$ and the indicator function $I_j(x_d)$ $(j = 0, 1, 2)$ is defined as:

$$I_j(x_d) = \begin{cases} 1, & \text{if there are } j \text{ Dirichlet boundaries} \\ & \text{perpendicular to } x_d \text{ axis,} \\ 0, & \text{otherwise.} \end{cases} \tag{14}$$

□

For example, in Fig. 3 (a), there is one Dirichlet boundaries perpendicular to x_1 axis, so $I_1(x_1) = 1$; there is no Dirichlet boundary perpendicular to x_2 axis, $I_0(x_2) = 1$. And in Fig. 3 (e), there are two Dirichlet boundaries perpendicular to x_1 and x_2 axes respectively, therefore $I_2(x_1) = I_2(x_2) = 1$ and the other indicator functions take value of zero.

It follows from Theorem 2 that the minimum eigenvalue of the grounded Laplacian is given in the following corollary.

Corollary 1: Consider the D-dimensional information graph $\mathbf{Z}_{n_1\times\cdots\times n_D}$ where D_0 is the number of axes in the information graph that have Dirichlet boundaries (either one or two) perpendicular to them. Without loss of generality, let these coordinates be $x_1, \ldots, x_{D_0}$. If $N_d \gg 1$ for $d = 1, \ldots, D_0$, then the minimum eigenvalue

$\lambda_{\min}$ of the grounded Laplacian L_g is $O(\frac{1}{N_p^2})$, where $p := \arg\min_{d=1,\ldots,D_0} N_d$. □

Proof of Corollary 1. Consider the following case first: each of the first D_0 coordinates that have Dirichlet boundaries perpendicular to them have exactly one Dirichlet boundary. That is, $I_1(x_d) = 1$, $I_0(x_d) = I_2(x_d) = 0$ for $d = 1, \ldots, D_0$, and $I_0(x_d) = 1$, $I_1(x_d) = I_2(x_d) = 0$ for $d > D_0$. We get from Theorem 2 that

$$\lambda_\ell = 2D - 2\sum_{d=1}^{D_0} \cos\frac{(2\ell_d - 1)\pi}{2N_d + 1} - 2\sum_{d=D_0+1}^{D} \cos\frac{(\ell_d - 1)\pi}{N_d}.$$

The minimum among them is obtained by setting $\ell_d = 1$ for $d = 1, \ldots, D$, which gives

$$\lambda_{\min} = 2D_0 - 2\sum_{d=1}^{D_0} \cos\frac{\pi}{2N_d + 1}.$$

Since $N_d \gg 1$ for each d in the summation, we use $\cos x = 1 - x^2/2 + O(x^4)$ when $|x| \ll 1$ to obtain $\cos\frac{\pi}{2N_d+1} = 1 - \frac{\pi^2}{8N_d^2} + O(\frac{1}{N_d^4})$. Hence,

$$\lambda_{\min} = \sum_{d=1}^{D_0} \left(\frac{\pi^2}{4N_d^2} + O(\frac{1}{N_d^4})\right) \Rightarrow$$

$$\frac{\pi^2}{4N_p^2} + O(\frac{1}{N_p^4}) \le \lambda_{\min} \le \frac{D_0\pi^2}{4N_p^2} + O(\frac{1}{N_p^4}). \quad (15)$$

It is straightforward (though tedious) to repeating these calculations for the other cases (when the number of Dirichlet boundaries is not exactly one). We see from these calculations that the asymptotic dependence on N_p does not change from that in (15), only the coefficients differ among the different cases. This proves the result. ■

The next result combines the ones establishes so far to give an explicit formula for the stability margin of the formation.

Theorem 3: Let $\lambda_{\min}$ be the minimum eigenvalue of the grounded Laplacian L_g. The stability margin of the closed loop with N vehicles is

$$S = \frac{\lambda_{\min} b}{2}, \quad (16)$$

when $N_p \gg 1$, where N_p is defined in Corollary 1. □

Proof. From Theorem 1, it follows that the eigenvalues of state matrix $\mathbf{A}$, denoted by s, satisfy:

$$s^2 + \lambda_\ell b s + \lambda_\ell k = 0, \quad (17)$$

where $\lambda_\ell \in \sigma(L_g)$. From Theorem 2, we see that λ_ℓ is positive. Since $k > 0$ and $b > 0$, it follows that $\mathbf{A}$ is Hurwitz. Moreover, it follows from (17) that the least stable eigenvalue of $\mathbf{A}$, denoted by s_1^+, is given by:

$$s_1^+ = -\frac{\lambda_{\min} b}{2}\left(1 + \sqrt{1 - \frac{4k}{\lambda_{\min} b^2}}\right) \quad (18)$$

It follows from Corollary 1 that it is possible to make $\lambda_{\min}$ arbitrarily small by choosing N_p sufficiently large. We choose N_p large enough so that $\lambda_{\min} < \frac{4k}{b^2}$, which makes the term inside the square root in (18) negative. Following the definition of stability margin, we obtain

$$S = |Re(s_1^+)| = \frac{\lambda_{\min} b}{2}.$$

■

IV. Scaling Laws for Stability Margin

The main result of the paper is the following.

Theorem 4: Consider an N-vehicle formation with a D-dimensional information graph $\mathbf{Z}_{n_1 \times \cdots \times n_D}$, with vehicle dynamics (1) and control law (2), where D_0 is the number of axes in the information graph that have Dirichlet boundaries (either one or two) perpendicular to them. The closed-loop stability margin is given by

$$S = \frac{\pi^2 b}{2}\sum_{d=1}^{D_0}\left[\frac{I_1(x_d)}{4} + I_2(x_d)\right]\frac{1}{N_d^2}, \quad (19)$$

when $N_p \gg 1$, where N_p is defined in Corollary 1. □

Proof. Follows from Theorem 3 and Corollary 1. □

The implication of the theorem is discussed next.

A. Stability Margin with Square Information Graphs

In interpreting Theorem 4, it is useful to start with the special case of a *square* information graph, which has equal number of real vehicles/nodes along each coordinate axis in the drawing of the information graph.

Definition 4: An information graph is said to be *square* if $N_1 = N_2 = \ldots = N_D$. ■

For a square information graph, $N_d = N^{\frac{1}{D}}$ for every d, which gives us the following corollary to Theorem 4.

Corollary 2: The closed-loop stability margin for a vehicle formation with D-dimensional square information graph has the asymptotic trend $S = O(\frac{1}{N^{2/D}})$, when $N^{1/D} \gg 1$. □

This result shows that for a square information graph, stability margin approaches 0 with an asymptotic decay of $O(1/N^{2/D})$, irrespective of on which boundary (boundaries) the lead vehicles are present. The stability margin scales as $O(1/N^2)$ in an 1D information graph, as $O(1/N)$ in a 2D information graph, and as $O(1/N^{2/3})$ in a 3D information graph. Thus, *for the same control gains and arrangements of lead vehicles, increasing the dimension of the information graph improves the stability margin significantly*. In practice, increasing the dimension of the graph may require a communication network with long range connections in the physical space. The reason is that two nodes that are neighbors in the information graph need not be physically close. Thus, one can strike a trade-off between the cost of long-range communication vis-a-vis the improvement in stability margin.

B. Stability Margin with Non-square Information Graphs

For ease of description, we describe the idea for non-square information graph with only one Dirichlet boundary. The information graph with other boundary configurations can be interpreted in a similar manner. The following corollary is immediate from Theorem 4.

Corollary 3: Suppose only one of the boundaries of the information graph has lead vehicles, and let this boundary be perpendicular to x_1 axis, without loss of generality. Then, $S = \frac{\pi^2 b}{8}\frac{1}{N_1^2}$. □

It follows from this result that by choosing the structure of the information graph in such a way that N_1 increases slowly in relation to N, the loss of the stability margin as a function of N can be slowed down. In fact, when N_1 is held at a constant value independent of N, the stability margin is a constant independent of the total number of vehicles!

More generally, if $N_1 = O(N^c)$, where $c \in [0, 1]$ is a fixed constant, it follows from Corollary 3 that $S = O(1/N^{2c})$ as $N \to \infty$. If $c < \frac{1}{D}$, the resulting reduction of S with N is slower than that obtained for a square lattice; cf. Corollary 2. This shows that within the class of D dimensional lattices (for a fixed D), certain information graphs provide better scaling of the stability margin than others. The price one pays for improving stability margin by reducing N_1 is an increase in the number of lead vehicles. This is because the number of lead vehicles, N_r, is related to N_1 (under the assumptions in Corollary 3) by $N_r = N/N_1$. There is thus a trade-off between improved stability margin and cost of having a large number of lead vehicles.

It is important to stress that not all non-square graphs are advantageous. For example, if $N_1 = O(N)$, which means N_2 through N_D are $O(1)$, it follows from Corollary 3 that the stability margin is $S = O(1/N^2)$. This is the same trend as in a 1-D information graph. In this case, we can say that the D dimensional information graph effectively behaves as a one dimensional graph.

Figure 4 shows a few examples of information graph that are relevant to the discussion above. Figure 5 provides numerical corroboration of the discussion above. It is clear from the figure that the prediction from Corollary 3 and Theorem 4 match very well with numerical computed eigenvalues of the state matrix $\mathbf{A}$.

V. Conclusion and Discussion

We study the problem of distributed control of a large network of double-integrator agents with D-dimensional information graph. We showed that the stability margin scales as $O(1/N^{2/D})$ for a D-dimensional square information graph. Therefore, increasing the dimension of the information graph can improve the stability margin by a considerable amount. For non-square information graph, the stability margin can be made independent of the number of agents by choosing the "aspect ratio" appropriately.

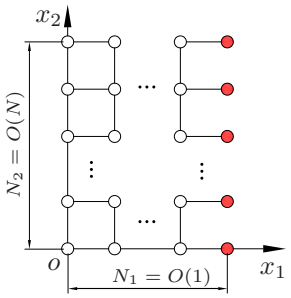

(a) Non-square information graph, $S = O(1)$

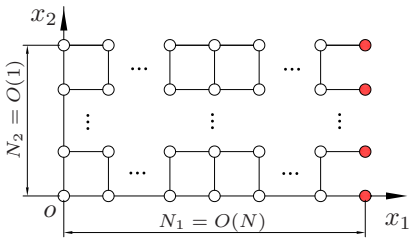

(b) Non-square information graph, $S = O(1/N^2)$

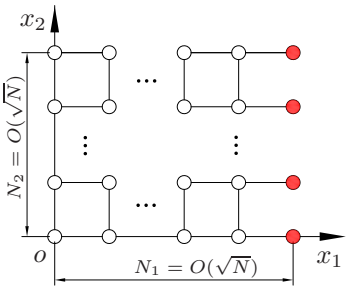

(c) Square information graph, $S = O(1/N)$

Fig. 4. (a) A $2D$ information graph in which the first dimension is held constant, resulting in a stability margin that is independent of N, $S = O(1)$. (b) A $2D$ information graph that is "asymptotically" 1D (as $N \to \infty$) since the size of the first dimension increases linearly with N, resulting in a stability margin scaling law $S = O(1/N^2)$, which is the same as that with an 1D information graph. (c) A $2D$ information graph in which both sides are of length $O(\sqrt{N})$, for which we have $S = O(1/N)$.

However, it should be taken into account that increasing the dimension of the information graph or choosing a beneficial aspect ratio may require long range communication or entail an increase in the number of lead vehicles. Thus, a larger stability margin can be achieved by designing the graph (and its boundary conditions) appropriately, but that may be accompanied by the increased cost of long-range communication or large number of lead vehicles. These results are therefore useful to the designer in making trade-offs between performance and cost in designing information exchange architectures for decentralized control.

Our results for square D-lattices are complementary to those of [14], in which the effect of graph dimension on the response of the closed loop to stochastic disturbances is quantified in terms of "microscopic" and "macroscopic" measures. It was shown in [14] that for $D > 5$, these performance measures become independent of N, while for smaller D, the performance becomes worse without bound as the number of vehicles increase. In contrast, we showed

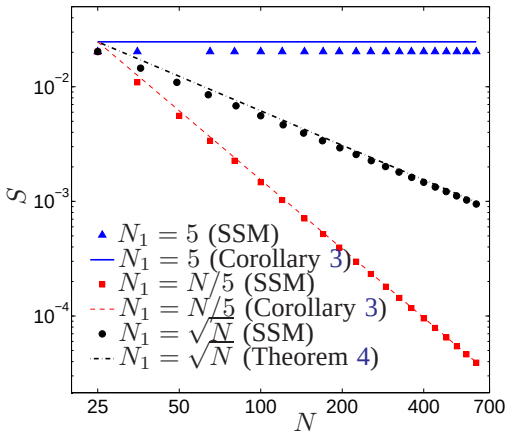

Fig. 5. Stability margin for a vehicle formation with information graphs of various "shapes" as shown in Figure 4. The legend "SSM" means computed from the "state space model" (6), which is presented in Section II. For the first case, $N_1 = 5$ and $N_2 = N/5$. Corollary 3 predicts that in this case $S = O(1)$ even as $N \to \infty$. In the second case, $N_2 = 5$ and $N_1 = N/5$, which leads to $S = O(1/N^2)$. The third case is that of a square information graph, $N_1 = N_2 = \sqrt{N}$, which leads to $S = O(1/N)$. Corollary 3 and Theorem 4 predict the stability margin quite accurately in each of the cases. The control gains used in all the calculations are $k = 0.1$ and $b = 0.5$.

that the stability margin decays to 0 as N increases in every D. Though the decay is slower for larger D, it is never independent of N. To achieve a size-independent stability margin, the graph needs to be non-square. Since the analysis of [14] is done in the spatial Fourier domain, it is not clear if non-square lattices with boundaries can be handled in that framework.

References

[1] P. M. Ludwig, "Formation control for multi-vehicle robotic minesweeping," Master's thesis, Naval postgraduate school, 2000.

[2] E. Wagner, D. Jacques, W. Blake, and M. Pachter, "Flight test results of close formation flight for fuel savings," in *AIAA Atmospheric Flight Mechanics Conference and Exhibit*, 2002, AIAA-2002-4490.

[3] H. G. Tanner and D. K. Christodoulakis, "Decentralized cooperative control of heterogeneous vehicle groups," *Robotics and autonomous systems*, vol. 55, no. 11, pp. 811–823, 2007.

[4] J. K. Hedrick, M. Tomizuka, and P. Varaiya, "Control issues in automated highway systems," *IEEE Control Systems Magazine*, vol. 14, pp. 21 – 32, December 1994.

[5] Y. Zhang, E. B. Kosmatopoulos, P. A. Ioannou, and C. C. Chien, "Autonomous intelligent cruise control using front and back information for tight vehicle following maneuvers," *IEEE Transactions on Vehicular Technology*, vol. 48, pp. 319–328, January 1999.

[6] P. Barooah, P. G. Mehta, and J. P. Hespanha, "Mistuning-based decentralized control of vehicular platoons for improved closed loop stability," *IEEE Transactions on Automatic Control*, vol. 54, no. 9, pp. 2100–2113, September 2009.

[7] P. Seiler, A. Pant, and J. K. Hedrick, "Disturbance propagation in vehicle strings," *IEEE Transactions on Automatic Control*, vol. 49, pp. 1835–1841, October 2004.

[8] S. K. Yadlapalli, S. Darbha, and K. R. Rajagopal, "Information flow and its relation to the stability of the motion of vehicles in a rigid formation," in *Proceedings of the 2005 American Control Conference*, June 2005, pp. 1853–1858.

[9] P. Barooah and J. P. Hespanha, "Error amplification and disturbance propagation in vehicle strings," in *Proceedings of the 44th IEEE conference on Decision and Control*, December 2005.

[10] M. R. Jovanović and B. Bamieh, "On the ill-posedness of certain vehicular platoon control problems," *IEEE Transactions on Automatic Control*, vol. 50, no. 9, pp. 1307 – 1321, September 2005.

[11] S. K. Yadlapalli, S. Darbha, and K. R. Rajagopal, "Information flow and its relation to stability of the motion of vehicles in a rigid formation," *IEEE Transactions on Automatic Control*, vol. 51, no. 8, August 2006.

[12] B. Bamieh, M. R. Jovanović, P. Mitra, and S. Patterson, "Effect of topological dimension on rigidity of vehicle formations: fundamental limitations of local feedback," in *Proceedings of the 47th IEEE Conference on Decision and Control*, Cancun, Mexico, 2008, pp. 369–374.

[13] H. Hao, P. Barooah, and P. G. Mehta, "Distributed control of two dimensional vehicular formations: stability margin improvement by mistuning," in *ASME Dynamic Systems and Control Conference*, October 2009.

[14] B. Bamieh, M. Jovanovic, P. Mitra, and S. Patterson, "Coherence in large-scale networks: Dimension dependent limitations of local feedback," 2009, submitted to IEEE Trans. Aut. Cont. [Online]. Available: http://engineering.ucsb.edu/~bamieh/

[15] F. Chung, "Spectral graph theory," Regional Conference Series in Mathematics, Providence, R.I., 1997.

[16] J. J. P. Veerman, G. Lafferriere, J. S. Caughman, and A. Williams, "Flocks and formations," *Journal of Statistical Physics*, vol. 121, pp. 901–936, 2005.

[17] W. Yueh, "Eigenvalues of several tridiagonal matrices," *Applied Mathematics E-Notes*, vol. 5, pp. 66–74, 2005.

Appendix

Proof of Theorem 2. The proof proceeds by an induction method. We'll study the 1D and 2D cases in detail, and induce the D-dimensional case from the hypothesis for $(D-1)$-dimensional information graph. Before we proceed further, let's first look at the eigenvalues of three special $n \times n$ tridiagonal matrices R_a, S_a and T_a. Matrix R_a has the form:

$$R_a = \begin{bmatrix} (a-1) & -1 & & & \\ -1 & a & -1 & & \\ & \ddots & \ddots & \ddots & \\ & & -1 & a & -1 \\ & & & -1 & (a-1) \end{bmatrix}. \qquad (20)$$

The eigenvalues of R_a are given by (see [17]):

$$\lambda_\ell = a - 2\cos\frac{(\ell-1)\pi}{n}, \quad \ell = 1, 2, \ldots, n. \qquad (21)$$

And S_a has the following form:

$$S_a = \begin{bmatrix} (a-1) & -1 & & & \\ -1 & a & -1 & & \\ & \ddots & \ddots & \ddots & \\ & & -1 & a & -1 \\ & & & -1 & a \end{bmatrix}. \qquad (22)$$

The eigenvalues of S_a are given by (see [17]):

$$\lambda_\ell = a - 2\cos\frac{(2\ell-1)\pi}{2n+1}, \quad \ell = 1, 2, \ldots, n. \qquad (23)$$

Matrix T_a is a tridiagonal Toeplitz matrix,

$$T_a = \begin{bmatrix} a & -1 & & & \\ -1 & a & -1 & & \\ & \ddots & \ddots & \ddots & \\ & & -1 & a & -1 \\ & & & -1 & a \end{bmatrix}. \qquad (24)$$

The eigenvalues of T_a are standard results:

$$\lambda_\ell = a - 2\cos\frac{\ell\pi}{n+1}, \quad \ell = 1, 2, \ldots, n. \tag{25}$$

For a $1D$ information graph, there are 3 possible boundary configurations: 1) there is no reference vehicle (This is the trivial case, since there is a zero eigenvalue); 2) there is only one reference vehicle on one end of the $1D$ lattice; 3) there is one reference vehicle on each end of the $1D$ lattice. For these three scenarios, the grounded Laplacians are respectively R_2, S_2 and T_2, their eigenvalues are given by (21), (23) and (25) respectively.

Combining these results, we obtain the formula for the eigenvalues of the grounded Laplacian $L_g^{(1)}$ for a general $1D$ information graph,

$$\begin{aligned}\lambda_{\ell_1} =& 2 - 2\Big[I_0(x_1)\cos\frac{(\ell_1-1)\pi}{N_1} + I_1(x_1)\cos\frac{(2\ell_1-1)\pi}{2N_1+1} \\ &+ I_2(x_1)\cos\frac{\ell_1\pi}{N_1+1}\Big],\end{aligned} \tag{26}$$

where $\ell_1 = 1, 2, \ldots, N_1$ and $I_j(x_1)$ $(j = 0, 1, 2)$ is the indicator function defined in (14).

For a $2D$ information graph, there are 5 nontrivial possible boundary configurations, as shown in Figure 3. It can be shown that the general grounded Laplacian $L_g^{(2)}$ can be expressed as:

$$L_g^{(2)} = I_{N_2} \otimes L_g^{(1)} + M \otimes I_{N_1}, \tag{27}$$

where the $L_g^{(1)}$ is the grounded Laplacian for the $1D$ lattice with boundary condition of $L_g^{(2)}$ on the x_1 axis and M is the grounded Laplacian for the $1D$ lattice with boundary of $L_g^{(2)}$ on the x_2 axis. The dimension of $L_g^{(1)}$ and M are $N_1 \times N_1$ and $N_2 \times N_2$ respectively. For example, the grounded graph Laplacian for the information graph shown in Fig. 3 (a) can be shown as:

$$L_g^{(2)} = I_4 \otimes S_2 + R_2 \otimes I_3 \tag{28}$$

where S_2 is defined in (22) with dimension 3×3 and R_2 is defined in (20) with dimension 4×4.

Following Theorem 1, the eigenvalues of $L_g^{(2)}$ are given by

$$\begin{aligned}\lambda_{\ell_1,\ell_2} &= \sigma(L_g^{(2)}) = \bigcup_{\lambda_{\ell_2}\in\sigma(M)} \{\sigma(L_g^{(1)} + \lambda_{\ell_2} I_{N_1})\}, \\ &= \bigcup_{\lambda_{\ell_2}\in\sigma(M)} \{\sigma(L_g^{(1)}) + \lambda_{\ell_2}\}, \\ &= \lambda_{\ell_1}(L_g^{(1)}) + \lambda_{\ell_2}(M), \\ &= 4 - 2\sum_{d=1}^{2}\Big[I_0(x_d)\cos\frac{(\ell_d-1)\pi}{N_d} + \\ &I_1(x_d)\cos\frac{(2\ell_d-1)\pi}{2N_d+1} + I_2(x_d)\cos\frac{\ell_d\pi}{N_d+1}\Big],\end{aligned} \tag{29}$$

where $\ell_1 = 1, 2, \ldots, N_1$ and $\ell_2 = 1, 2, \ldots, N_2$.

Now, we assume the general formula for the eigenvalues of the grounded Laplacian $L_g^{(D-1)}$ of a $(D-1)$-dimensional information is given by

$$\begin{aligned}\lambda_{\ell_1,\ldots,\ell_{D-1}} = 2(D-1) - 2\sum_{d=1}^{D-1}\Big[&I_0(x_d)\cos\frac{(\ell_d-1)\pi}{N_d} \\ &+ I_1(x_d)\cos\frac{(2\ell_d-1)\pi}{2N_d+1} + I_2(x_d)\cos\frac{\ell_d\pi}{N_d+1}\Big].\end{aligned} \tag{30}$$

For a D-dimensional information graph, the grounded Laplacian $L_g^{(D)}$ can be shown to be expressed as:

$$L_g^{(D)} = I_{N_D} \otimes L_g^{(D-1)} + M \otimes I_{N_1 N_2 \cdots N_{D-1}}, \tag{31}$$

where the $L_g^{(D-1)}$ is the grounded Laplacian for the $(D-1)$-dimensional lattice with boundary condition of $L_g^{(D)}$ on the x_1 to x_{D-1} axes and M is the grounded Laplacian for the $1D$ lattice with boundary of $L_g^{(D)}$ on the x_D axis. The dimension of $L_g^{(D-1)}$ and M are $(N_1 N_2 \cdots N_{D-1}) \times (N_1 N_2 \cdots N_{D-1})$ and $N_D \times N_D$ respectively. From Theorem 1, the eigenvalues of $L_g^{(D)}$ are given by

$$\lambda_{\ell_1,\ldots,\ell_D} = \lambda(L_g^{(D-1)}) + \lambda(M) \tag{32}$$

Using the induction hypothesis in (30), we have

$$\begin{aligned}\lambda_{\ell_1,\ldots,\ell_D} &= 2(D-1) - 2\sum_{d=1}^{D-1}\Big[I_0(x_d)\cos\frac{(\ell_d-1)\pi}{N_d} \\ &+ I_1(x_d)\cos\frac{(2\ell_d-1)\pi}{2N_d+1} + I_2(x_d)\cos\frac{\ell_d\pi}{N_d+1}\Big] \\ &+ 2 - \Big[I_0(x_D)\cos\frac{(\ell_D-1)\pi}{N_D} \\ &+ I_1(x_D)\cos\frac{(2\ell_D-1)\pi}{2N_D+1} + I_2(x_D)\cos\frac{\ell_D\pi}{N_D+1}\Big] \\ &= 2D - 2\sum_{d=1}^{D}\Big[I_0(x_d)\cos\frac{(\ell_d-1)\pi}{N_d} \\ &+ I_1(x_d)\cos\frac{(2\ell_d-1)\pi}{2N_d+1} + I_2(x_d)\cos\frac{\ell_d\pi}{N_d+1}\Big].\end{aligned} \tag{33}$$

To prove the eigenvalues $\lambda_{\ell_1,\ldots,\ell_D}$'s are all positive, we start from the formula of eigenvalues given in (33). Under the assumption that there is at least one Dirichlet boundary in the D-dimensional information graph, without loss of generality, let it be perpendicular to x_1, thus we have $I_1(x_1) = 1$, $I_0(x_d) = 1$ $(d = 2, \ldots, D)$ and the other indicator functions take values of zero. The minimum eigenvalue becomes:

$$\lambda_{\min} = \lambda_{1,\ldots,1} = 2 - 2\cos\frac{\pi}{2N_1+1} > 0$$

Moreover, the more Dirichlet boundaries it has than before, the bigger the minimum eigenvalue is. ■